High-Performance Multifunctional TiO2 Nanowire Ultrafiltration Membrane with a Hierarchical Layer Structure for Water Treatment

ARTICLE *in* ADVANCED FUNCTIONAL MATERIALS · DECEMBER 2009

Impact Factor: 11.81 · DOI: 10.1002/adfm.200901435

4 AUTHORS, INCLUDING:

Xiwang Zhang
Monash University (Australia)
78 PUBLICATIONS **1,899** CITATIONS
SEE PROFILE

Darren Delai Sun
Nanyang Technological University
189 PUBLICATIONS **5,970** CITATIONS
SEE PROFILE

ADVANCED FUNCTIONAL MATERIALS
www.afm-journal.de

High-Performance Multifunctional TiO_2 Nanowire Ultrafiltration Membrane with a Hierarchical Layer Structure for Water Treatment

By *Xiwang Zhang,* Tong Zhang, Jiawei Ng,* and *Darren Delai Sun**

A novel, multifunctional TiO_2 nanowire ultrafiltration (UF) membrane with a layered hierarchical structure is made via alkaline hydrothermal synthesis, followed by a filtration and hot-press process. The TiO_2 UF membrane has high surface porosity (21.3%) and pore size values around 20 nm. The membrane possesses multifunctional capabilities under UV irradiation, such as anti-fouling, anti-bacterial, concurrent separation, and photocatalytic oxidation. The unique properties of the membrane indicate its potential in applications for environmental purification.

1. Introduction

Membrane technologies have been wildly applied in water treatment, dairy, food, pharmaceutical, bioengineering, chemical, nuclear-energy, and electronic industries. The membrane separation of gases and liquids can often be more economical and energy effective than traditional separation methods, such as distillation or absorption.[1–4] Recently, ceramic membranes have attracted considerable attention due to their excellent thermal, chemical, and mechanical stability as compared to polymeric membranes.[5–7] Ceramic membranes generally have an unsymmetrical layered structure, consisting of two layers: a supporting and a functional layer (separation layer), while some consist of an additional intermediate layer. The selectivity and permeability of the membranes are controlled principally by characteristics of the functional layer, such as the pore size, thickness, and porosity. The functional layers are usually fabricated via coating sols of metal hydrates on the supporting layers. However, formation of pinholes and cracks within the membrane usually occur during the drying and calcination process.[2] Membrane flux is proportional to the pressure difference across the membrane. As a result, membranes need to able to withstand high pressure and flux, which are inevitable in ultrafiltration (UF) or nanofiltration (NF) processes.

Since the first reports on carbon nanotubes in 1991 by S. Iijima[8] and WS_2 nanotubes in 1992 by R. Tenne,[9] various 1D inorganic materials in the form of nanotubes,[10] nanowires,[11] and nanofibers,[12] have been extensively fabricated. Recently, research focus has been placed on the synthesis of 2D materials, such as films, sheets, and membranes using 1D materials, as well as exploring their potential applications.[13–17] These 2D materials are mostly in the form of nanomeshes, since 1D materials are prone to interweaving each other. Theoretically, the mesh structure, as conjugated by 1D materials, should be most efficient for filtration since it provides increased selectivity and flux, due to its high surface porosity and pore density.[2,18] Ke et al. lately fabricated a ceramic membrane via a spin-coating and calcination method. The resulting membrane has a pore size of 60 nm and consists of a titanate fiber intermediate layer and alumina fiber separation layer.[2,19] Their study clearly showed that the fiber separation layer offers high flux with excellent selectivity. Among the materials used for the preparation of ceramic membranes, titanium dioxide (TiO_2) is unique due to its excellent performance under UV irradiation on mineralization of a variety of organic compounds.[20] A large number of research studies have been carried out to fabricate TiO_2 membranes.[5,21–24] It has been proven that TiO_2 membranes can provide concurrent filtration and photocatalytic oxidation.[21,22] In our previous study,[23] a free-standing TiO_2 nanowire microfiltration (MF) membrane was successfully fabricated. The permeability test results showed that the membrane produces higher membrane flux with a narrower membrane pore size distribution. However to date, fabrication of highly permeable TiO_2 UF membranes still remains a challenge.

In this study, we designed a new type of TiO_2 UF membrane consisting of two different dimensions of TiO_2 nanowires: ultrafine (diameter: 10 nm) and large (diameter: 20–100 nm) nanowires. The two kinds of nanowires are labeled TNW_{10} and TNW_{20}, in accordance to their respective diameters. The TNW_{10} layer serves as the functional layer while the TNW_{20} layer is laid as the supporting layer. The as-synthesized membrane offers three major advantages: 1) high permeability and high selectivity; 2) concurrent photocatalytic oxidation and separation; and 3) anti-fouling and anti-bacterial capabilities.

2. Results and Discussion

2.1. Membrane Characterization

Typical transmission electron microscopy (TEM) images of the two as-prepared nanowires, TNW_{10} and TNW_{20}, are shown in

[*] Dr. X. Zhang, Prof. D. D. Sun, T. Zhang, J. Ng
School of Civil and Environmental Engineering
Nanyang Technological University
639798 Singapore (Singapore)
E-mail: xwzhang@ntu.edu.sg; ddsun@ntu.edu.sg

DOI: 10.1002/adfm.200901435

Figure 1A and B, respectively. TNW_{20} has a diameter of approximately 20–100 nm and a length of several micrometers, while TNW_{10} measures about 10 nm in diameter and several hundred of nanometers in length. Both nanowires could form different porous structures due to the incongruity of their diameters as shown in Figure 1C. Figure 1D shows a digital photo of the as-prepared TiO_2 membrane before calcination. The as-prepared membrane is flexible and can be shaped as desired by calcination.

The TiO_2 membrane was prepared with a two-step process: membrane filtration of the TiO_2 nanowire suspension, and a hot press process to compact the membrane formed (see Supporting Information, Fig. S1). During filtration of TNW_{20} and TNW_{10} suspensions in sequence, the supporting and functional layers of the TiO_2 membrane were formed by the interwoven TNW_{20} and TNW_{10}, respectively. This fabrication method allows the construction of layers of randomly oriented nanowires (LRONW) as shown in Figure 2. The thicknesses of the supporting and functional layers were easily controlled by adjusting suspension volumes of TNW_{20} and TNW_{10} for filtration. The LRONW structure of TNW_{20} produced pore sizes of 50–150 nm as shown in Figure 2C and F and can be categorized as a microfiltration (MF) membrane.[23] Further reduction in pore size using TNW_{20} is difficult due to its relatively large diameter. It is known that the diameter of the precursor nanowires determines the pore size of the resulting LRONW membrane.[2] However, the LRONW of TNW_{20} can serve as substrate or support on which ultrathin nanowire TNW_{10} can be deposited to form another LRONW stratum of smaller pore size since TNW_{10} nanaowires are much thinner and shorter than TNW_{20} nanowires. A homogeneous TNW_{10} membrane must be thick enough to withstand the filtration driving force and to enhance the mechanical strength of the membrane since it can be rather brittle from the fact that short TNW_{10} nanowires are used. The hierarchical layered structure of the TNW_{10}/TNW_{20} membrane bestowed increased mechanical strength and permeability to the membrane because the membrane flux is inversely proportional to the thickness of the functional layer. Figure 2E shows the cross-section of the hierarchical TiO_2 nanowire membrane. It is observed that both TNW_{10} and TNW_{20} layers bound strongly to form a closely wound and tight network of nanowires, as each nanowire systematically weaved into the adjoining layers. From the magnified cross-sectional image (Fig. 2B) of TNW_{10}, it can be seen that the functional layer was compact with tightly interwoven nanowires.

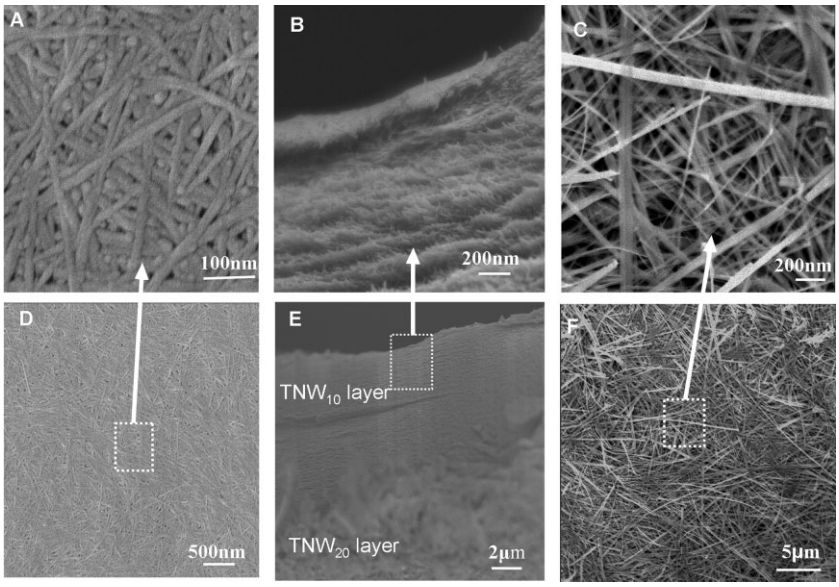

Figure 2. Construction of the hierarchical layers of the TiO_2 UF membrane. A) High-resolution upper-surface SEM image of the TNW_{10} functional layer. B) The cross-section of the TNW_{10} functional layer. C) High-resolution SEM image of the bottom surface of the TNW_{20} supporting layer. D) SEM image of the upper surface of the TNW_{10} functional layer. E) The cross-section of the TiO_2 UF membrane. F) SEM image of the bottom surface of the TNW_{20} supporting layer.

Figure 2D shows the surface of the TNW_{10} functional layer. The surface was relatively flat, and no cracks were detected. The pore size of LRONW of TNW_{10} ranges from 10 to 25 nm, as shown in Figure 2A.

The crystal structures and phase compositions of the as-prepared and calcined membranes were identified by X-ray diffraction (XRD), with peaks shown in Figure 3. TNW_{20} and TNW_{10} originated from $Na_2Ti_nO_{2n+1}$ and $K_2Ti_nO_{2n+1}$, respectively, which were synthesized through the alkaline-hydrothermal process. The formation mechanism of $Na_2Ti_nO_{2n+1}$ has been reported previously in relevant references.[25,26] During the alkaline-hydrothermal reaction, some of the Ti−O−Ti bonds of precursors are broken to form a six-coordinated monomer, $[Ti(OH)_6]^{2-}$. This monomer is highly unstable and thus prone to forming original nuclei. $Na_2Ti_nO_{2n+1}$ is

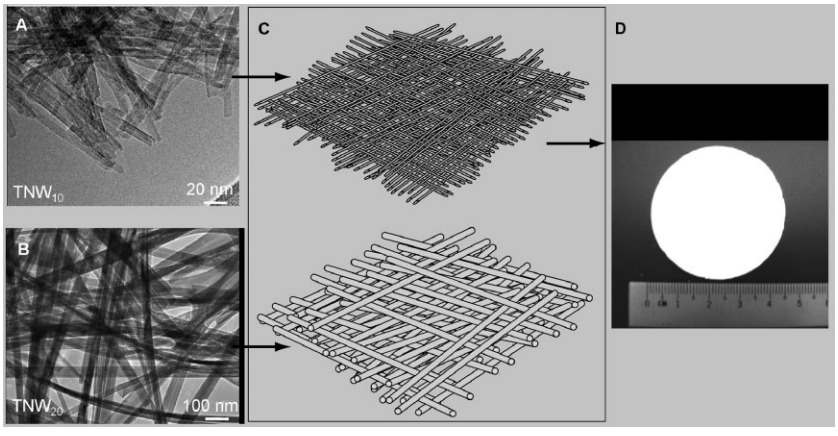

Figure 1. Components of the hierarchical layer of the TiO_2 nanowire UF membrane. A) TEM image of TNW_{10}, B) TEM image of TNW_{20}, C) Schematic profiles of the TiO_2 nanowire UF membrane. D) Digital photo of the TiO_2 nanowire UF membrane.

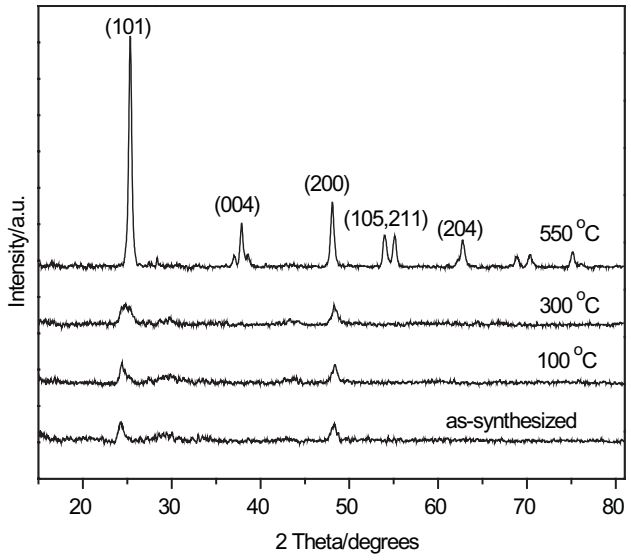

Figure 3. Powder XRD pattern of TiO_2 nanowire UF membrane: as-prepared (i.e., uncalcined) and after calcination at different temperatures (100, 300, and 550 °C).

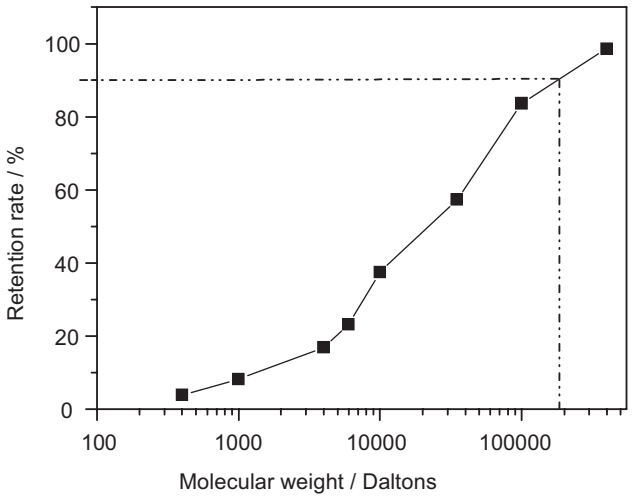

Figure 4. Retention rates of PEG and PEO of different molecular weights by the TiO_2 nanowire UF membrane.

subsequently grown around the nuclei formed. The difference in morphological rates of each crystallographic direction, leads to the formation of 1D nanowires. The diameter of a single $Na_2Ti_nO_{2n+1}$ nanowire is about 20 nm. However, several nanowires can readily bond together to form a large nanowire with a diameter of more than 100 nm. The formation mechanism of $K_2Ti_nO_{2n+1}$ is similar to that of $Na_2Ti_nO_{2n+1}$, but the diameter of $K_2Ti_nO_{2n+1}$ nanowires (10 nm) is markedly smaller than $Na_2Ti_nO_{2n+1}$. Moreover, no binding of $K_2Ti_nO_{2n+1}$ nanowires was observed; hence sizes are very uniform, leading to a narrow pore size distribution of the functional layer. When the nanowires of $Na_2Ti_nO_{2n+1}$ and $K_2Ti_nO_{2n+1}$ were immersed and washed using a dilute acidic solution, Na^+ and K^+ ions were replaced by H_3O^+ ions, resulting in $H_2Ti_nO_{2n+1}$ nanowires. It was found that complete removal of sodium and potassium ions from the as-prepared sample can be achieved by ultrasonic washing at room temperature with 0.2 M HCl or HNO_3. Calcination at 550 °C fully dehydrated and converted the $H_2Ti_nO_{2n+1}$ nanowires into pure anatase TiO_2, as shown in Figure 3.

2.2. Membrane Evaluation

The molecular weight cut-off (MWCO) is often used to characterize the separation property of a UF membrane, and it is defined as the molecular weight of a component with 90% retention. The MWCO of the TiO_2 nanowire membrane was evaluated by filtering different molecular weights of polyethylene glycol (PEG) and polyethylene oxide (PEO) in aqueous solution. Figure 4 shows the retention rates of PEG and PEO of varying molecular weights by the TiO_2 nanowire membrane. The molecular weight of PEO with 90% retention was about 200 kDa, which means that the MWCO of the TiO_2 nanowire membrane is classified at around 200 000. The corresponding pore size of the LRONW membrane is around 20 nm, according to the relationship between pore size and MWCO.[27] It was consistent with the value observed directly from scanning electron microscopy (SEM) images. The surface porosity of the membrane was measured to be 21.3%, and the pore density was calculated to be 6.7×10^{10} cm^{-2}. To evaluate permeability of the membrane, the permeate flux was measured using boiled water and the results was 12.2 L m^{-2} min^{-1} bar^{-1} (1 bar = 10^3 kPa. The flux rate achieved is significantly greater than flux rates of commercial ceramic membranes with similar MWCO and is more than 13 times the flux rate as reported in previous literature.[28]

2.3. Photocatalytic Activity

The photocatalytic activity of the TiO_2 nanowire membrane was first evaluated by photocatalytic oxidation of methylene blue (MB) under UV irradiation (254 nm). The TiO_2 nanowire membrane with a mark of MB (1.0×10^{-4} mol L^{-1}) was exposed to UV light as shown in Figure 5. A glass fiber (ADVANTEC, GC-50, 0.45 μm) with the same mark was used for comparison. After 30 min of irradiation, no remarkable change was observed to the mark on the glass fiber membrane. In contrast, the mark on the TiO_2 nanowire membrane disappeared, which concludes that the MB on the TiO_2 membrane surface was totally oxidized. Under UV irradiation, TiO_2 can be excited to generate highly oxidative species, holes (h^+) and hydroxyl radicals (OH ·).[20,29] Previous investigations indicate that these species can degrade organic matter—a group of the most commonly identified foulants in surface water filtration.[30,31] Therefore, fouling of the TiO_2 membrane would be alleviated if a UV lamp was used to irradiate the membrane during filtration. The TiO_2 nanowire membrane would simultaneously execute an anti-fouling function, which has been verified in our previous study.[23] Figure 6 shows the variation of permeate flux of the TiO_2 nanowire membranes during filtration of 10 mg L^{-1} humic acid (HA) with and without UV irradiation. All the membrane pores in the TiO_2 nanowire membrane are linked with each other, such that the

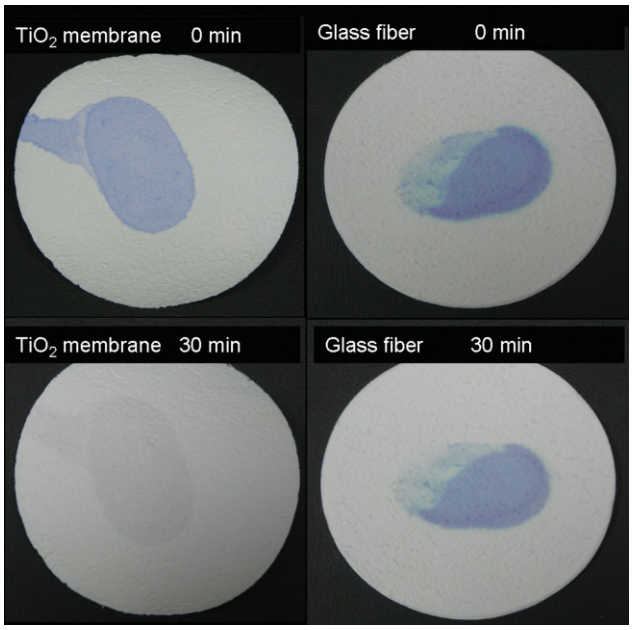

Figure 5. Evaluation of the photocatalytic activity of the TiO_2 nanowire UF membrane in comparison to a glass fiber membrane.

pores will not be easily blocked. It was proved that the permeate flux of the membrane without UV irradiation declined by less than 50% after 10 h of filtration. Under UV irradiation, foulants were destroyed by photocatalytic oxidation, hence mitigating membrane fouling. It was observed that the permeate flux was kept almost constant throughout the 10 h of filtration. Moreover, the removal rate of HA by the TiO_2 nanowire membrane was dramatically promoted to almost 100% by the UV irradiation from 66.5% without UV irradiation.

Apart from chemical pollution, biological pollution (in relation to bacteria and viruses) has aroused increasing attention due to the health risks involved. Bacteria cells are typically sized from 0.5 to 5 μm, whereas cells of viruses measure from 50 nm onwards.[2,30]

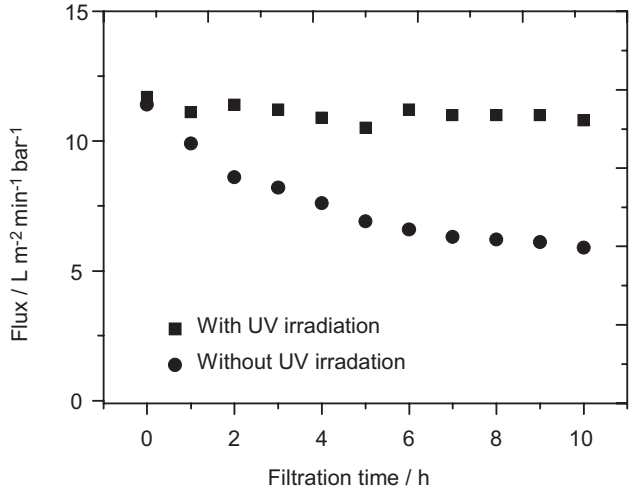

Figure 6. Changes in membrane flux of the TiO_2 nanowire UF membrane during filtration of 10 mg L^{-1} HA. Transmembrane pressure: 0.8 bar.

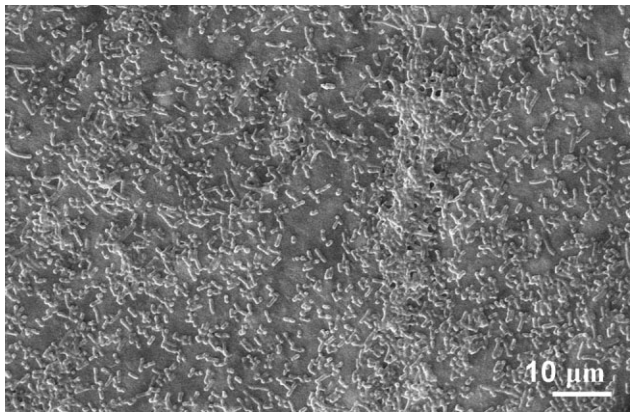

Figure 7. SEM image of the used TiO_2 nanowire UF membrane after filtration of the *E. coli* solution.

Since the pores of the TiO_2 nanowire membrane is measured at 20 nm, bacteria and viruses from air and water should be effectively filtered out. To verify the membrane capacity in rejecting viruses and waterborne pathogens, an indicative bacteria, *E. coli*, was filtered in an aqueous medium. The membrane was characterized after filtration using SEM and Figure 7 showed the image of the membrane surface. It is apparent that the *E. coli* cells were retained on the membrane surface because they are larger than the membrane pores. It was found that no *E. coli* cells were present in the filtrate, indicating that *E. coli* was totally rejected by the membrane (Supporting Information, Fig. S2). The used membrane was irradiated under a UV light source with a wavelength of 365 nm, and the kill ratio of *E. coli* on the membrane as a function of irradiation time was detected. An identical experiment was conducted using an Al_2O_3 UF membrane (Whatman, 0.02 μm) for comparison purposes. The amount of live *E. coli* on the membrane declined dramatically and more than 99.9% destruction of the *E. coli* colonies was attained after 60 min of irradiation as shown in Figure 8. In contrast, less than half of the amount of *E. coli* cells on the Al_2O_3 membrane was inactivated

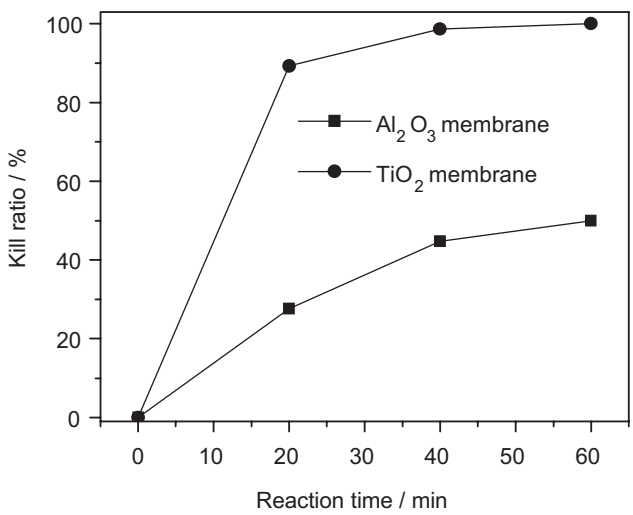

Figure 8. Inactivation of *E. coli* by the TiO_2 nanowire UF membrane.

under identical experimental conditions. The inactivation of *E. coli* on Al_2O_3 membrane was attributed to UV direct irradiation because Al_2O_3 has no any photocatalytic activity.

3. Conclusions

The antibacterial property of the TiO_2 nanowire membrane provides a wide array of advantages when compared to the existing water treatment systems. Firstly, there is no need for an additional disinfection unit, which is currently required in conventional water treatment plants. In addition to allowing capital investments and operating overheads to be substantially reduced, the major health issues of concern to the public—such as the formation of disinfection by-products (DBPs)—can also be rectified. DBPs are unavoidable in traditional disinfection processes due to the reactions between chemical disinfectants and natural organic matter (NOM), which are prevalent in surface waters. DBPs have drawn increasing attention over the years since most of them are suggested to be carcinogenic. In addition, biofouling of membranes has also been prevented to a large extent. Some anaerobic bacteria are prone to growing on membrane surfaces and insides of membrane pores, where the latter is considered one of the main causes of irreversible membrane fouling. The antibacterial property of the TiO_2 membrane is able to inhibit growth of anaerobic bacteria, thus averting issues of membrane biofouling.

In this study, a hierarchical TiO_2 UF membrane was fabricated using two types of TiO_2 nanowires, 20–100 nm TNW_{20} and 10 nm TNW_{10}. TNW_{20} forms the supporting layer of the membrane, which provides mechanical strength, while TNW_{10} forms the functional layer, which provides excellent permeability and separation properties. The TiO_2 nanowire UF membrane has excellent performance in photodegradation and anti-fouling tests. When the multifunctional nanowire UF membrane was applied in a typical filtration process, organic and biological pollutants were destroyed and inactivated under UV irradiation. Concurrently, membrane fouling was also controlled adequately by suppressing growth of membrane foulants. As a result, we believe that this nanowire membrane will have a huge impact on membrane development, and its use in environmental applications is highly promising.

4. Experimental

The fabrication of the two types of TiO_2 nanowires via hydrothermal synthesis is based on previously published literature [26,32]. In a typical experiment, 10 M NaOH and TiO_2 P25 were used to synthesize TNW_{20}, and the hydrothermal reaction was conducted at 180 °C for 3 days. The product was collected after the hydrothermal reaction and washed using HCl or HNO_3 (0.2 M) and deionized water with ultrasonic assistance. TNW_{10} was fabricated by the same procedure, except that NaOH was replaced by KOH. TNW_{20} and TNW_{10} were individually dispersed in a surfactant (0.05 wt% F-127) solution, to form two suspensions. The suspensions of TNW_{20} and TNW_{10} were sonicated using an ultrasonic finger for 5 min to achieve a homogeneous dispersion. The TNW_{20} suspension was first filtered on a vacuum-filtration setup with a glass filter (ADVANTEC, GC-50, 0.45 μm) to form the supporting layer, and thereafter, filtering of the TNW_{10} suspension resulted in the formation of the functional layer. Residual surfactant left in the membrane was subsequently washed away using distilled water. A membrane, consisting of a layered structure, was formed on the glass filter upon filtration of the suspensions. After drying at 105 °C, a free-standing membrane remained after removal of the glass filter. The membrane was then pressurized under 5 bar at 120 °C on a hot press to achieve compaction, before being calcined at 550 °C.

The morphological structure of TNW_{20} and TNW_{10} and the membrane were examined using a transmission electron microscope (TEM, JEOL 2010) and a field-emission scanning electron microscope (FESEM, JEOL 6340). The crystal structure and phase composition were analyzed using a powder X-ray diffraction system (XRD, Bruker AXS D8 advance). The surface porosity and pore density were detected from KCl diffusion measurements [33]. The MWCO of the TiO_2 nanowire membrane was determined by filtering PEG of different molecular weights (0.4, 1, 4, 6, 10, and 35 kDa) and PEO with molecular weights of 100 and 400 kDa. The PEG and PEO solutions (50 mL of each) were filtered using a Millipore UF filtration setup. The concentrations of PEG in the feed and filtrate were determined by a Shimadzu TOC-VCSH total organic carbon (TOC) analyzer. The retention rates (R) of different PEGs and PEOs by the nanowire membrane were determined via the following equation:

$$R = \left(1 - \frac{TOC_{\text{filtrate}}}{TOC_{\text{feed}}}\right) \times 100\% \quad (1)$$

where TOC_{filtrate} and TOC_{feed} are the respective TOC concentrations in the filtrate and feed of PEG and PEO solutions.

The photocatalytic activity of the TiO_2 nanowire membrane was evaluated using two variants of model pollutants, namely MB and HA, both of which were used as purchased. An Upland 3SC9 pen-ray lamp (254 nm) was used as the UV light source. The concurrent photocatalytic oxidation and separation properties of the TiO_2 nanowire UF membrane were evaluated by filtering an HA solution (10 mg L^{-1}) under 0.8 bar on a laboratory-scale setup, as described in our previous paper [23]. The concentration of HA in solution was detected by monitoring the absorbance of sample at 436 nm on a UV–visible spectrophotometer.

The antibacterial property of the membrane was evaluated by assessing the inactivation of *E. coli*. Water (5 mL) containing *E. coli* (10^6 CFU mL^{-1}) was filtered by the TiO_2 nanowire membranes. A total of four TiO_2 nanowire membranes were employed, and they were concurrently irradiated by an Upland 11SC-1L pen-ray lamp (365 nm). Each membrane was drawn at an interval of 20 min to transfer the live *E. coli* cells onto an agar plate. To enumerate the live *E. coli* cells, the membrane was washed using a sodium phosphate buffer solution, such that the total volume collected from the washed membrane was 5 mL. These 5 mL of washed solution was then further diluted by a factor of 100–10000. The solution was subsequently streaked onto an agar plate, prepared using a broth culture medium, to support the growth of *E. coli*. Manual counting of colonies per unit surface area of the agar plate was conducted to determine the established *E. coli* cell counts. Similar experiments were conducted using an Al_2O_3 UF membrane (Whatman, 0.02 μm) for comparison. Sampling was carried out in triplicate, and results were averaged to minimize experimental discrepancies involved in the biological experiments.

Acknowledgements

The authors would like to acknowledge the Singapore Environment & Water Industry (EWI) Development Council (MEWR 651/06/166) and the Public Utilities Board of Singapore for their research grant and support for this work. We would also like to thank FACTS for the characterization analysis of the membrane. Supporting Information is available online from Wiley InterScience or from the author.

Received: July 31, 2009
Published online: November 9, 2009

[1] D. S. Sholl, J. K. Johnson, *Science* **2006**, *312*, 1003.
[2] X. B. Ke, H. Y. Zhu, X. P. Gao, J. W. Liu, Z. F. Zheng, *Adv. Mater.* **2007**, *19*, 785.
[3] A. Van den Berg, M. Wessling, *Nature* **2007**, *445*, 726.
[4] M. A. Shannon, P. W. Bohn, M. Elimelech, J. G. Georgiadis, B. J. Marinas, A. M. Mayes, *Nature* **2008**, *452*, 301.
[5] H. Choi, A. C. Sofranko, D. D. Dionysious, *Adv. Funct. Mater.* **2006**, *16*, 1067.
[6] R. M. de Vos, H. Verweij, *Science* **1998**, *279*, 1710.
[7] J. K. Holt, H. G. Park, Y. Wang, M. Stadermann, A. B. Artyukhin, C. P. Grigoropoulos, A. Noy, O. Bakajin, *Science* **2006**, *312*, 1034.
[8] S. Iijima, *Nature* **1991**, *354*, 56.
[9] R. Tenne, L. Margulis, M. Genut, G. Hodes, *Nature* **1992**, *360*, 444.
[10] M. Remscaronkar, *Adv. Mater.* **2004**, *16*, 1497.
[11] M. Law, J. Goldberger, P. Yang, *Annu. Rev. Mater. Res.* **2004**, *34*, 83.
[12] D. Li, Y. Xia, *Adv. Mater.* **2004**, *16*, 1151.
[13] Z. Wu, Z. Chen, X. Du, J. M. Logan, J. Sippel, M. Nikolou, K. Kamaras, J. R. Reynolds, D. B. Tanner, A. F. Hebard, A. G. Rinzler, *Science* **2004**, *305*, 1273.
[14] M. Zhang, S. Fang, A. A. Zakhidov, S. B. Lee, A. E. Aliev, C. D. Williams, K. R. Atkinson, R. H. Baughman, *Science* **2005**, *309*, 1215.
[15] G. Gu, M. Schmid, P. W. Chiu, A. Minett, J. Fraysse, S. R. Gyu-tae Kim, M. Kozlov, E. Munoz, R. H. Baughman, *Nat. Mater.* **2003**, *2*, 316.
[16] M. Endo, H. Muramatsu, T. Hayashi, Y. A. Kim, M. Terrones, M. S. Dresselhaus, *Nature* **2005**, *433*, 476.
[17] Y. Wang, G. Du, H. Liu, D. Liu, S. Qin, N. Wang, C. Hu, X. Tao, J. Jiao, J. Wang, Z. L. Wang, *Adv. Funct. Mater.* **2008**, *18*, 1131.
[18] W. Dong, A. Cogbill, T. Zhang, S. Ghosh, Z. R. Tian, *J. Phys. Chem. B* **2006**, *110*, 16819.
[19] X. B. Ke, Z. F. Zheng, H. W. Liu, H. Y. Zhu, X. P. Gao, L. X. Zhang, N. P. Xu, H. Wang, H. J. Zhao, J. Shi, K. R. Ratinac, *J. Phys. Chem. B* **2008**, *112*, 5000.
[20] M. R. Hoffmann, S. T. Martin, W. Choi, D. W. Bahnemann, *Chem. Rev.* **1995**, *95*, 69.
[21] S. P. Albu, A. Ghicov, J. M. Macak, R. Hahn, P. Schmuki, *Nano Lett.* **2007**, *7*, 1286.
[22] X. Zhang, A. J. Du, P. Lee, D. D. Sun, J. O. Leckie, *Appl. Catal. B* **2008**, *84*, 262.
[23] X. Zhang, A. J. Du, P. Lee, D. D. Sun, J. O. Leckie, *J. Membr. Sci.* **2008**, *313*, 44.
[24] H. Choi, E. Stathatos, D. D. Dionysiou, *Appl. Catal. B* **2006**, *63*, 60.
[25] Y. Wang, G. Du, H. Liu, D. Liu, S. Qin, N. Wang, C. Hu, X. Tao, J. Jiao, J. Wang, Z. L. Wang, *Adv. Funct. Mater.* **2008**, *18*, 1131.
[26] Z. Y. Yuan, B. L. Su, *Colloids Surf. A* **2004**, *241*, 173.
[27] T. Thorsen, *Water Sci. Technol.* **1999**, *40*, 105.
[28] M. Rajca, M. Bodzek, K. Konieczny, *Desalination* **2009**, *239*, 100.
[29] A. Fujishima, T. N. Rao, D. A. Tryk, *J. Photochem. Photobiol. A* **2000**, *1*, 1.
[30] X. Z. Li, H. Liu, L. F. Cheng, H. J. Tong, *Environ. Sci. Technol.* **2003**, *37*, 3989.
[31] C. Tang, Y. N. Kwon, J. O. Leckie, *J. Membr. Sci.* **2007**, *290*, 86.
[32] X. Zhang, J. H. Pan, A. J. Du, W. Fu, D. D. Sun, J. O. Leckie, *Water Res.* **2009**, *43*, 1179.
[33] M. Majumder, N. Chopra, R. Andrews, B. J. Hinds, *Nature* **2005**, *438*, 44.